J. T. Tuoriniemi and K. I. Juntunen. 2004. Nuclei in cooperation. Journal of Low Temperature Physics 135, pages 513-543.

# Nuclei in Cooperation

**Juha Tuoriniemi and Kirsi Juntunen**

*Low Temperature Laboratory, Helsinki University of Technology*
*PO.Box 2200, FIN-02015 HUT, Finland*

*We analyze and discuss two distinct resonance phenomena at high nuclear polarizations, which give independent experimental information about the exchange couplings, direct or indirect, between the nuclear spins in solids. In cases of more than one isotope with a nuclear spin, there is an isotopic-interference effect, sometimes referred to as a suppression-enhancement effect. Even in cases with just one spin species, one may observe harmonic lines of the ordinary Larmor resonance. By analyzing the shifts and intensities of the resonance lines as functions of the nuclear polarization, one can find the sign and magnitude of the exchange couplings. The focus of this paper is in experiments on nuclear magnetic ordering in pure metals. We present studies on copper, silver, rhodium, thallium, and gold, and discuss shortly our ongoing work on lithium.*

*PACS numbers: 76.60.-k, 76.60.Jx, 75.30.Et, 75.10.Jm.*

## 1. INTRODUCTION

### 1.1. Prologue

Nuclear magnets are the most predictable and clean systems, which exhibit spontaneous magnetic ordering. By no means does this make the problem of studying the ordered states trivial – not theoretically and, in particular, not experimentally.[1,2] Having a well characterized substance for such investigations is so invaluable, that it pays to take the trouble of exploring at extremely low temperatures the very same phenomena that are familiar from more ordinary electronic magnetism.

Nuclear spins in simple pure metals, which are otherwise magnetically inert, are for many reasons exemplary samples for such studies. There combine some of the most attractive properties of the other two distinct exten-

sively studied classes of nuclear magnets, by which we refer to the dynamically polarized nuclei in insulators[2,3] and to the diverse group of hyperfine enhanced nuclear magnets[4]. As in insulators, the interactions between the nuclear spins in ordinary metals are accurately known and can be calculated from first principles. Still, there are variations in the decisive characteristics among even the simplest metals to justify experiments on different materials without just repeating the same results all over again. This is because the pure dipolar interaction is accompanied by the indirect-exchange coupling mediated by the conduction electrons,[5] the strength of which may vary from overwhelming, as in gold or platinum, to nearly negligible, as in lithium or beryllium. Moreover, very interesting behavior can result when the two interaction mechanisms are of comparable magnitude, such as in copper.[6]

Nuclear magnetism in several simple metals has been investigated in our laboratory by SQUID-NMR techniques over a period of more than three decades under the keen superintendence and discreet but purposeful influence of Olli Lounasmaa. Due to his initiative some of these metals, first found to order antiferromagnetically in our laboratory, were subsequently studied by neutron diffraction in two broad European collaborations.[7]

In this article we shall not give any general overview of this work, large part of which was reviewed by Oja and Lounasmaa in 1997,[1] but shall focus on one particular aspect, which is, in fact, one of the foundation stones of this research: the exchange contribution to the nuclear spin-spin interactions.

Nuclei in cooperation produce two distinct resonance phenomena, one of which is observable at low magnetic fields only while the other one is brought about by finite polarization of the nuclei: the double-spin effect and the isotope effect, respectively. At high nuclear polarizations the exchange term modifies these effects, giving an opportunity to directly measure the relative strength of the exchange and dipolar forces. Although the indirect exchange can be calculated from the electronic band structure, see Ref. 1 and references therein, it is rewarding to have unbiased methods to check the validity of such cumbersome calculations.

In the following we shortly survey the earlier papers on this subject, present a coherent algebra applying to the analysis of both phenomena, show new detailed data on copper, reexamine some of the earlier measurements, and finally relate the discussion to our present studies on lithium metal.

## 1.2. Prior Art of the Methods

In order to ascertain the requirement of knowing accurately the interactions between the nuclear spins in metals, as stated at the beginning of the

introduction, methods for checking experimentally the presumed values have been pursued perpetually. The dipolar interaction is accurately known but the estimates for the indirect term are less rigorous and, therefore, deserve some special attention.

The early paper by Ekström *et al.*[8] introduced most of the concepts that we further develop to some extent here. The authors observed both the double-spin effect and the isotope effect on copper, for which they deduced a consistent magnitude of the indirect exchange.

Since then the same tools have been applied in studies of silver[9,10] and rhodium[11]. In silver the isotope effect was observed at both positive and negative absolute temperatures, but the weak double-spin effect was beyond resolution. Another manifestation of the exchange coupling was seen in the thermalization measurements of the isotopic lines in silver.[12] While rhodium has only one stable isotope, the corresponding effect does not exist at all, but the double-spin effect was nicely resolved at both positive and negative absolute temperatures.[11]

A peculiar line splitting observed at high nuclear polarizations in thallium[13] has been attributed to the isotope effect[14]. However by applying the appropriate parameters for thallium to the expressions derived below for the peak positions and intensities of the isotopic lines, one can show indisputably that the proposed splitting mechanism due to the two isotopes cannot be correct.

Currently, we are working on nuclear magnetism in lithium, but it is too early to include any data on this metal to the present paper. Nevertheless, the issues discussed here are ever so topical, when measurements on a new material are commenced.

## 2. THE MODEL

The following considerations are based on a simple general Hamiltonian $\mathcal{H} = \mathcal{H}_Z + \mathcal{H}_d + \mathcal{H}_J$ consisting of the Zeeman term, the dipolar term and the exchange term

$$\begin{cases} \mathcal{H}_Z = -hB_0 \sum_i \gamma_i I_i^z - hB_\perp e^{i2\pi ft} \sum_i \gamma_i I_i^x \\ \mathcal{H}_d = \frac{1}{2}\frac{\mu_0}{4\pi} h^2 \sum_{ij} \gamma_i\gamma_j [\mathbf{I}_i \cdot \mathbf{I}_j - 3(\mathbf{I}_i \cdot \hat{\mathbf{r}}_{ij})(\mathbf{I}_j \cdot \hat{\mathbf{r}}_{ij})]/r_{ij}^3 \\ \mathcal{H}_J = -\frac{1}{2} \sum_{ij} J_{ij} (\mathbf{I}_i \cdot \mathbf{I}_j) \end{cases} , \qquad (1)$$

respectively. The spins $\mathbf{I}_i$ with the gyromagnetic ratio $\gamma_i$ are exposed to an oscillatory (with the frequency $f$) excitation field $B_\perp$ perpendicular to the static magnetic field $B_0$. The dipolar term depends on the distance between the spins $r_{ij}$ and the exchange is defined by the scalar couplings $J_{ij}$.

It is useful to define two quantities representing the strength of the spin-spin couplings: the "dipolar frequency" $f_s = \mu_0 h\gamma^2\rho I$, where $\rho$ is the number density of the spins $I$, and the relative exchange parameter $R = \sum_j J_{ij} I/(hf_s)$. Since we allow two spin species with different gyromagnetic ratios, $\gamma_a$ and $\gamma_b$, we must keep track of the family of each of the coupled spins and thus have in fact three dipolar frequencies $f_{sa}$, $f_{sb}$, and $f_{sx}$ with $\gamma_a^2$, $\gamma_b^2$, and $\gamma_a\gamma_b$, respectively. In the following, however, we shall always replace $f_{sx}$ by either $\frac{\gamma_b}{\gamma_a} f_{sa}$ or by $\frac{\gamma_a}{\gamma_b} f_{sb}$ so that only the other two will appear in the formulations after all. Note that the indirect exchange coupling between any pair of spins scales as $J_{ij} \propto \gamma_i\gamma_j$ so that the individuality of the spin species does not influence $R$.[5]

The equations of motion for the spin operators, *e.g.* $\dot{I}_i^+ = -i[I_i^+, \mathcal{H}]/\hbar$ with $I^+ = I^x + iI^y$, result in the quantum mechanical equivalents of the Bloch equations. The full representation with all details is unnecessarily complicated, whereby we include in the discussions only the terms relevant for the effect under treatment in each case.

### 2.1. Double-Spin Effect

This effect is treated comprehensively in the papers by Ekström *et al.*[8] and by Moyland *et al.*[15] Nevertheless, we reproduce the basic algebra to demonstrate that both effects can be described on the same footing. Also, we show that it is important to acknowledge the difference in the line widths of the two modes. Such difference can make the double-spin effect practically unobservable, which changes crucially the conclusions about the situation in gold[15] and may be the reason for missing this effect in silver.

The single- and double-spin operators of interest are $I^+ = \sum_i I_i^+$ and $X = \frac{\mu_0}{4\pi} h\gamma^2 \sum_{ij} 3r_{ij}^{-3}\gamma_{ij}(\alpha_{ij} - i\beta_{ij}) I_i^+ I_j^+ / f_d$, where $\alpha_{ij}$, $\beta_{ij}$, and $\gamma_{ij}$ are the direction cosines of $r_{ij}$. The double-spin terms $I_i^+ I_j^+$ are scaled by the coupling frequency

$$f_d = \frac{\mu_0}{4\pi} h\gamma^2 [18 \sum_l r_{lj}^{-3}\gamma_{lj}(\alpha_{lj} - i\beta_{lj}) \sum_k r_{kl}^{-3}\gamma_{kl}(\alpha_{kl} - i\beta_{kl}) I_k^z I_l^z]^{1/2}, \qquad (2)$$

whose relevance becomes clear below, when writing down the matrix representation for the corresponding equations of motion.[8] It is of the same order of magnitude as the dipolar frequency, $f_d \sim f_s$, and scales for different substances basically as $\gamma^2\rho\sqrt{I(I+1)}$.[8,11,15] The uncoupled modes have the resonance frequencies

$$\begin{cases} f_1^0 = f_0 + \frac{3}{2}(L - D)pf_s \\ f_2^0 = 2f_0 + 2(L - D + R)pf_s \end{cases}, \qquad (3)$$

which, for polarized nuclei ($p = \langle I^z \rangle / I$), are shifted slightly from the genuine Larmor or double-Larmor frequencies $f_0$ or $2f_0$.[8,15] Here, $L = \frac{1}{3}$ is the Lorentz factor, and $D$ is the demagnetization factor of the specimen in the direction of the static field.

All necessary ingredients can be included into a compact matrix representation

$$\begin{pmatrix} f_1 & f_d \\ f_d & f_2 \end{pmatrix} \begin{pmatrix} \chi_\perp \\ X \end{pmatrix} = f \begin{pmatrix} \chi_\perp \\ X \end{pmatrix} + \begin{pmatrix} p f_s \\ 0 \end{pmatrix}, \tag{4}$$

where the perpendicular susceptibility $\chi_\perp(f) = \mu_0 M_\perp / B_\perp = \mu_0 h \gamma \rho \langle I^+ \rangle / B_\perp$ is the experimentally observed quantity proportional to the average precessing spin $\langle I^+ \rangle$ induced by the oscillatory excitation field $B_\perp$. Note that there is no direct excitation component (the rightmost vector) for $X$, as the external drive for it averages to zero over the lattice sites. This is, in fact, the reason that the double-line intensity decreases so rapidly as the function of the magnetic field, since it is actually the precessing individual spins, which drive the double-spin processes.

We include, somewhat phenomenologically, the line-width contributions $\delta_1$ and $\delta_2$ to the diagonal frequencies of the coupling matrix, *viz.*

$$\begin{cases} f_1 = f_1^0 - i\delta_1 \\ f_2 = f_2^0 - i\delta_2 \end{cases} . \tag{5}$$

The effect of these, usually overlooked, is to weaken the observability of the second harmonic line. They derive, of course, from the very same Hamiltonian that couples the spins to each other, and can be estimated by the method of moments.[16,17] The second moment of the primary line is determined by the dipolar interaction alone.[17] For polycrystal samples we have at $p \ll 1$

$$M_2 = \frac{\mu_0^2}{4\pi} h^2 \gamma^4 \frac{3I(I+1)}{5} \sum_j r_{ij}^{-6} . \tag{6}$$

The spacing sum depends to some extent on the lattice structure, but for most practical purposes we can evaluate $\frac{3}{20\pi} \sum_j r_{ij}^{-6} \approx 0.35\rho^2$. After some manipulation we obtain $\delta_1 \approx \alpha(1-p^2)\sqrt{M_2}$, where $\alpha \sim 1$ depends on the higher moments of the line.[2] The secondary line, on the other hand, is broadened by the exchange interaction, which appears in its second moment as a contribution proportional to $I(I+1)\sum_j J_{ij}^2/h^2$.[16] The line width can be expressed roughly as $\delta_2 \approx \delta_1 \sqrt{1+\beta R^2}$ with $\beta$ depending on the microscopic details but being of the order of unity. The full analysis of the moments of the secondary line is rather tedious[16] but the simplified expression above still reflects the most central result: an increasing difference between $\delta_2$ and $\delta_1$ is expected when the exchange-type interaction becomes the dominant

coupling mechanism between the spins. It is not at all granted that the harmonic line is detectable in such situations, as we shall show below.

The united spin system responds at the coupled mode frequencies found as the eigenvalues of the coupling matrix, *viz.*[8]

$$f_\pm = \frac{1}{2}[\ f_2 + f_1 \pm \sqrt{(f_2 - f_1)^2 + 4f_d^2}\ ]\ , \tag{7}$$

and the ratio of intensities, $I = \int_{-\infty}^{\infty} \chi_\perp$, of the two modes is[8,15]

$$I_+/I_- = 4f_d^2/|\ f_+ - f_- + \sqrt{(f_+ - f_-)^2 - 4f_d^2}\ |^2\ . \tag{8}$$

Due to the shifts of the resonance frequencies $f_1^0$ and $f_2^0$ from the Larmor and double-Larmor positions, see Eq. (3), the uncoupled lines appear to cross at $B_\times = \frac{1}{2}(-L + D - 4R)pf_s/\gamma$, where $f_1^0 = f_2^0$. However, at the vicinity of the line crossing there is repulsion between the modes and the coupled lines approach no closer than $f_+ - f_- = 2\sqrt{f_d^2 - \delta_d^2}$ with each other. Here we use $\delta_d = (\delta_2 - \delta_1)/2$. If $\delta_d \le f_d$, the two modes have equal strengths at the "anti-crossing" field, and the double-spin mode diminishes as $1/(B - B_\times)^2$ far from the crossing region. Note that above the crossing field, it is $f_+$ that corresponds to the double-spin mode, whereas below $B_\times$ it swaps to the $f_-$ mode. If $\delta_d > f_d$, the double-spin mode does not grow to equal intensity with the Larmor line at any value of the magnetic field. Even in the case $\delta_d \sim f_d$ it may be impossible to distinguish experimentally the two modes, as they are equally strong only when they fall practically on top of each other, and so the passing and interchange of the roles of the two modes at $B_\times$ may well go by unnoticed.

In above we did not carry along the notation for the different spin species, because the double-spin effect is observable at such low magnetic fields only, that the nuclear-isotope lines are usually unresolvable from each other. In principle, for two isotopes the double-spin line should split into three because of the three kinds of pairs, a-a, b-b, and a-b or b-a, possibly involved in the double-spin processes.

### 2.2. Isotope Effect

We use similar formalism, as above, to study the mutual influence between the spins of different isotopes. Some terms in the equations of motion, which cancel out for interacting pairs of equal spins, remain nonzero for unequal pairs and, therefore, the exchange interaction shows up already in the first order of spin operators.

This problem has been treated earlier by using the classical Bloch equations[8] and by using the perturbation theory in the operator formalism for an exchange-dominated case[12]. We show below that the problem can be analyzed consistently in terms of equations of motion for the spin operators. Such treatment can extend the validity of both the Bloch approach and the perturbation results, each of which is reproduced at the appropriate limits.

The single-spin operators for the two isotopes obey the following equations of motion:

$$\begin{cases} \frac{1}{2\pi}\dot{I_a^+} = -if_{aa}I_a^+ - i\frac{\gamma_b}{\gamma_a}f_{ab}I_b^+ + i\gamma_a B_\perp e^{i2\pi ft}I_a^z \\ \frac{1}{2\pi}\dot{I_b^+} = -if_{bb}I_b^+ - i\frac{\gamma_a}{\gamma_b}f_{ba}I_a^+ + i\gamma_b B_\perp e^{i2\pi ft}I_b^z \end{cases}, \tag{9}$$

where

$$\begin{cases} f_{aa} = f_{0a} + \frac{3}{2}(L-D)px_a f_{sa} + (L-D+R)\frac{\gamma_a}{\gamma_b}px_b f_{sb} - i\delta_{aa} \\ f_{bb} = f_{0b} + \frac{3}{2}(L-D)px_b f_{sb} + (L-D+R)\frac{\gamma_b}{\gamma_a}px_a f_{sa} - i\delta_{bb} \\ f_{ab} = \frac{1}{2}(L-D-2R)px_a f_{sa} + i\delta_{ab} \\ f_{ba} = \frac{1}{2}(L-D-2R)px_b f_{sb} + i\delta_{ba} \end{cases}. \tag{10}$$

We denote $I_n^\alpha = \sum_i^n I_i^\alpha$ with $\sum^n$, $n = a, b$ running only through the representative spin species, while $B_\perp$ is the amplitude of the excitation field at frequency $f$, orthogonal to the static field. The Larmor frequencies and the abundances of the two isotopes are $f_{0n}$ and $x_n$ with $n = a, b$, respectively. For simplicity, we assume $p_a = p_b = p$.

We can demonstrate, how the various terms come about, by looking at the exchange Hamiltonian $\mathcal{H}_J = -\sum_{i\neq j} J_{ij} I_i \cdot I_j = -\sum_{i\neq j} J_{ij}(I_i^z I_j^z + I_i^+ I_j^-)$. Both spin products $\sum_{i\neq j} J_{ij} I_i^\alpha I_j^\beta$ must be decomposed according to the spin families: $\sum_{i\neq j}^{aa} J_{ij} I_i^\alpha I_j^\beta + \frac{1}{2}\sum_i^a \sum_j^b J_{ij}(I_i^\alpha I_j^\beta + I_i^\beta I_j^\alpha) + \sum_{i\neq j}^{bb} J_{ij} I_i^\alpha I_j^\beta$. The contributions for equal pairs cancel out, because, for example, the average $\langle[\sum_{i\neq j}^{aa} J_{ij} I_i^z I_j^z, I_a^+]\rangle = 2hpx_a R f_{sa} I_a^+$ is exactly the opposite of the adjoining term $\langle[\sum_{i\neq j}^{aa} J_{ij} I_i^+ I_j^-, I_a^+]\rangle = -2hpx_a R f_{sa} I_a^+$. However, the "zz"-cross component $\langle[\sum_i^a \sum_j^b J_{ij} I_i^z I_j^z, I_a^+]\rangle = hpx_b R\frac{\gamma_a}{\gamma_b} f_{sb} I_a^+$ is not cancelled by $\langle[\frac{1}{2}\sum_i^a \sum_j^b J_{ij} I_i^- I_j^+, I_a^+]\rangle = -hpx_a R\frac{\gamma_b}{\gamma_a} f_{sa} I_b^+$, because the precessing spin component is that of the other spin species. The last two terms appear as the $R$-factors in $f_{aa}$ and $f_{ab}$. The commutators with $I_b^+$ result in the corresponding terms of $f_{bb}$ and $f_{ba}$, respectively. When the Zeeman and dipole Hamiltonians are treated similarly, we finally obtain the coupling frequencies of Eq. (10).

The presence of the foreign spins contribute to the line widths, which forces us to write down four different $\delta$'s. These can be evaluated much in a similar way as phrased above, although the full expressions become fairly

unhandy. Some general observations can be made, though. The straight widths $\delta_{nn}$ are constructed as follows:[17] i) Equal spins contribute to the line width principally through the dipolar coupling, simply weighted by their corresponding abundance $x_n$. ii) Dipolar coupling between unlike spins contributes only by a factor $\frac{2}{3}x_n$. iii) The exchange between unlike spins broadens the line by an additional factor $\sim x_n R/\sqrt{n_n}$, where $n_n$ is the number of nearest neighbors. (We assume that the exchange interaction decays rapidly enough to justify including nearest neighbors only.) iv) The total width squared is the sum of independent contributions squared.

Using the principles above, we obtain

$$\delta_{aa}^2 \approx (x_a\delta_a)^2 + (x_b\delta_b)^2(\frac{4}{9} + R^2/n_n) \tag{11}$$

and $\delta_{bb}$ for the isotope $b$ correspondingly. $\delta_a$ and $\delta_b$ represent the single-spin widths equivalent to those obtained from Eq. (6). The evaluation of the "cross widths" $\delta_{ab}$ and $\delta_{ba}$ is basically similar resulting in

$$\delta_{ab}^2 \approx (x_a\delta_a)^2(\frac{1}{9} + R^2/n_n) \tag{12}$$

and $\delta_{ba}$ correspondingly.

To be consistent, also the contributions $\delta_{aa}I_a^+$ and $\frac{\gamma_b}{\gamma_a}\delta_{ab}I_b^+$ should be summed up as squares, but this would result in less transparent nonlinear equations of motion. On the basis of some numerical analysis of such nonlinear cases we consider the proposed form of Eqs. (9) and (10) as an adequate approximation to this problem. We remind, that all line-width contributions, including the single-isotope widths $\delta_n$, were expressed as rather coarse estimates leaving some space for adjustments according to actually measured line shapes. Note that the sign of the width contribution is irrelevant when their squares are considered. This is why the proper sign assessment for the cross widths in Eq. (6) is opposite to the straight widths.

The linear equations of motion can be molded to the matrix representation

$$\begin{pmatrix} f_{aa} & f_{ab} \\ f_{ba} & f_{bb} \end{pmatrix} \begin{pmatrix} \chi_{\perp a} \\ \chi_{\perp b} \end{pmatrix} = f \begin{pmatrix} \chi_{\perp a} \\ \chi_{\perp b} \end{pmatrix} + \begin{pmatrix} px_a f_{sa} \\ px_b f_{sb} \end{pmatrix}, \tag{13}$$

with the susceptibilities $\chi_{\perp n} = \mu_0 h\gamma_n x_n \rho\langle I_n^+\rangle/B_\perp$. We find the eigenfrequencies, formally nearly identically to Eq. (7), as

$$f_\pm = \frac{1}{2}[\ f_{aa} + f_{bb} \pm \sqrt{(f_{aa} - f_{bb})^2 + 4f_{ab}f_{ba}}\ ]. \tag{14}$$

The term proportional to $f_{sa}f_{sb}$ of the product $f_{ab}f_{ba}$ in Eq. (14) results in increasing repulsion of the two NMR peaks as the polarization grows up.

On the other hand, the product of the cross widths $\delta_{ab}\delta_{ba}$ in $f_{ab}f_{ba}$ give rise to attractive displacement of the lines, remaining down to $p = 0$, consistent with the perturbation analysis by Oja *et al.*[12] The latter effect is important primarily in metals with $|R| > 1$, such as silver or thallium, whereas in copper with $R = -0.42$ we may set $\delta_{ab} = \delta_{ba} = 0$ without any appreciable impairment of the results.

The equations for the line intensities become somewhat complicated, partly because there are now source terms for both components in Eq. (13). It is useful to find the contributions of both the separate isotopes, $\chi_{\perp a}$ and $\chi_{\perp b}$, and also of the two coupled modes $\chi_{\perp +}$ and $\chi_{\perp -}$. The superposition of either pair, which sum up equivalently, is observed in the real measurement and, in practice, the individual contributions may be difficult to separate when the two modes become very close to each other.

We obtain

$$\chi_{\perp a}(f) = \frac{px_a f_{sa}(f_+ - f_{aa}) - px_b f_{sb} f_{ab}}{(f_+ - f_-)(f_- - f)} - \frac{px_a f_{sa}(f_- - f_{aa}) - px_b f_{sb} f_{ab}}{(f_+ - f_-)(f_+ - f)} \tag{15}$$

and, of course, a similar expression for $\chi_{\perp b}$ with all $a$'s and $b$'s interchanged. The first terms of $\chi_{\perp a}$ and $\chi_{\perp b}$ so written assimilate to $\chi_{\perp -}$, while the second terms sum up to $\chi_{\perp +}$. Now, both spin species respond at both frequencies $f_+$ and $f_-$. It can be seen that one breed has a positive peak at both frequencies but the other one has opposite polarities of the two peaks. Consequently, there is constructive interference of the isotopes at one mode and destructive interference at the other mode. Therefore, this phenomenon is also called the suppression-enhancement effect. Which one of the modes, $f_+$ or $f_-$, is amplified, depends on the sign and magnitude of the exchange constant $R$, which is exactly the parameter of interest here.

The relative intensity can be written as

$$I_+/I_- = \left| \frac{F_1(f_+ - f_-) - F_2(f_{bb} - f_{aa}) + p(x_a f_{sa} f_{ba} + x_b f_{sb} f_{ab})}{F_1(f_+ - f_-) + F_2(f_{bb} - f_{aa}) - p(x_a f_{sa} f_{ba} + x_b f_{sb} f_{ab})} \right| \tag{16}$$

with

$$\begin{cases} F_1 = (x_a f_{sa} + x_b f_{sb})/2 \\ F_2 = (x_a f_{sa} - x_b f_{sb})/2 \end{cases} . \tag{17}$$

In the discussion above, we have neglected the influence of the higher moments of the lines, which, however, may be important under some circumstances. The third order terms, $M_3 \propto p(1 - p^2)$, vanish at low and high polarization but make the lines asymmetric at intermediate region. The higher odd orders have the same tendency. The fourth order terms,

$M_4 \propto (1-p^2)(1-\eta p^2)$, (as well as higher even orders) vanish at high polarization but are influential at low $p$ where they suppress the tails of the lines making them often appear more like Gaussian in shape.[2]

## 3. THE METALS

We examine a number of previously published studies on several elemental metals and present some new improved data on copper. In all cases consistent results are obtained using the formalism introduced above.

### 3.1. Copper

Copper displays beautifully both of the effects discussed in this article. The strength of the indirect exchange is comparable to that of the dipolar interaction, so that its influence is easily observed at high nuclear polarizations. The double-spin effect shows up clearly without being smeared by exchange broadening of the harmonic line. Two isotopes exist, $^{63}$Cu and $^{65}$Cu with $x_{63} = 0.69$ and $x_{65} = 0.31$, with $\gamma_{63} = 11.30$ MHz/T and $\gamma_{65} = 12.10$ MHz/T, and with $I_{63} = I_{65} = \frac{3}{2}$.

The most accurate experimental determination of the exchange parameter $R = -0.42 \pm 0.05$ of Cu is based on observing the effects being discussed.[8] We have produced new data on copper with an improved signal to noise ratio as a side product of our ongoing studies on lithium metal, while our lithium samples have been capsuled by copper foils cooled down together with the actual specimens. The sample shape is different from what Ekström *et al.* used and therefore the demagnetization factors differ. We estimate $D = 0.09 \pm 0.01$ on the basis of the dimensions of our slab-shaped sample, which consisted of about 2 mm thick bunch of 24 long foils 50 $\mu$m each with a width of about 8 mm. The static field was usually oriented along the second longest side of the specimen. Some complications may arise because the demagnetization field is not exactly uniform across the rectangular and stripy cross section of the sample.

The specimen was cooled in a double-stage nuclear-demagnetization cryostat[18] in a similar fashion as described in Ref. 8. Typically, we polarized the sample in 2–3 T at about 0.3 mK for 2–3 h and the demagnetization was carried out in 10–15 min. The short polarization period ensured that selectively the copper nuclei were polarized, as lithium has more than an order of magnitude larger Korringa constant than copper. This was important mainly for the measurements in low fields (double-spin effect), where the NMR lines of the two metals overlap with each other.

In a typical measurement after the demagnetization, the excitation frequency, chosen from the range 10–150 kHz, was kept constant and the magnetic field was swept back and forth across the resonances, while the spin system was warming up towards equilibrium with the lattice. One sweep took usually about five minutes and the nuclei relaxed back to the lattice temperature in a few hours. The polarization scale for the runs at different frequencies could be found at equilibrium with the lattice in the respective measuring field range. In the static fields applied, 1–13 mT, and at the lattice temperatures around 0.3 mK, the equilibrium polarization was of the order of 1%, and the NMR signals were still easily and accurately measurable. Any other value of polarization could then be found by comparing the integrated area under the absorption curve of the recorded dynamic susceptibility. However, good agreement with the initial polarization estimated on the basis of the temperature, field, and duration of the polarization and demagnetization phases was found only at the higher measuring frequencies ($> 100$ kHz), while at lower frequencies (and thus lower fields) the area of the absorption peaks appeared to grow less than linearly with polarization. This is not totally unexpected as the assumed simple linear relationship is valid only in fields much greater than the local field ($B_{loc} = 0.34$ mT for copper); clear deviations were observed still at few milliteslas. Consequently, in the low-field runs the polarization had to be calculated from the estimated initial value and the relaxation time. The lattice temperature $T_e$, measured by a Pt-NMR thermometer, could be checked independently by the spin-lattice relaxation time $\tau_1$ of the copper nuclei through the Korringa relation $T_e = \kappa_{Cu}\tau_1$. No serious discrepancies were found in any of the runs, although, as expected, the relaxation speeds up somewhat at the lowest fields.

The double-spin resonance was observed very clearly at frequencies between 10–30 kHz, see Fig. 1. The data at 11 and 13 kHz display passing of the two modes with the minimum separation of 0.23 mT, in fair agreement with the results of Ekström *et al.*[8] The closest separation is smaller than mere repulsion of the lines would allow ($\sim 0.30$ mT), which is an indication of a clear difference in the widths of the two modes, as pointed out already, but not fully explained, in Ref. 8. The suggested line widths squared differ by $\Delta = \sqrt{\delta_2^2 - \delta_1^2} \approx R\sqrt{M_2} \approx 4$ kHz, which is of proper magnitude to account for the close passing of the two lines.

It is important to note, that the line width of the double-spin mode seen experimentally is not the same as $\delta_2$, because the double-spin mode can be observed only indirectly through the coupling with the single-spin precession. In fact, the computed spectra display more or less equal line widths for the two modes, and to explain the differences clearly observed in the experiment, one must include some cross-coupling widths to the coupled

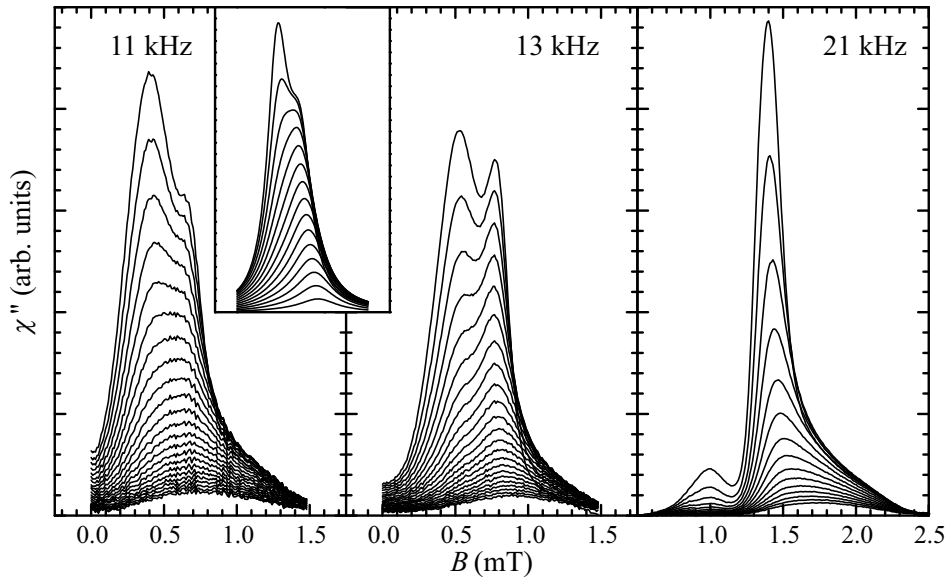


Fig. 1. Measured resonance shapes of copper at $f = 11$, 13, and 21 kHz, where the double-spin mode is very clear. The nuclear polarization varies between about $p = 0.04$–$0.6$ in each run. The inset: calculated spectra at $f = 11$ kHz between $p = 0.05$–$0.75$ with increments of 0.05.

equations of motion, as we did in the analysis of the isotope effect.

The computed behavior at the line crossing is shown in the inset of Fig. 1. Qualitatively the evolution is similar to what we observe, but the actual line shapes deviate clearly from the Lorentzian lines produced by the linear equations.

Quantitative analysis of the intensities of the two modes is troublesome because of the large overlap of the lines. We fitted the data with Lorentzian shapes, where, in addition, the width was allowed to vary in a Gaussian manner as the function of field. To be more specific, we used for fitting the basic function

$$\chi"(B) = \frac{\chi_0 A^2 \Gamma(B)}{(B - B_L)^2 + \Gamma(B)} \tag{18}$$

with

$$\Gamma(B) = \Gamma_L^2 e^{-\ln 2[(B-B_G)/\Gamma_G]^2} \ . \tag{19}$$

This way it is possible to interpolate the line shape from fully Lorentzian ($\Gamma_G \to \infty$ and $A = 1$) to pure Gaussian ($A = B_L \to \infty$ and $\Gamma_L = 1$), as is necessary due to the changes in the measured line shapes, as the spin system was warming up. Further, by allowing a (small) difference between the center frequencies of the Lorentzian and Gaussian parts ($B_L \neq B_G$),

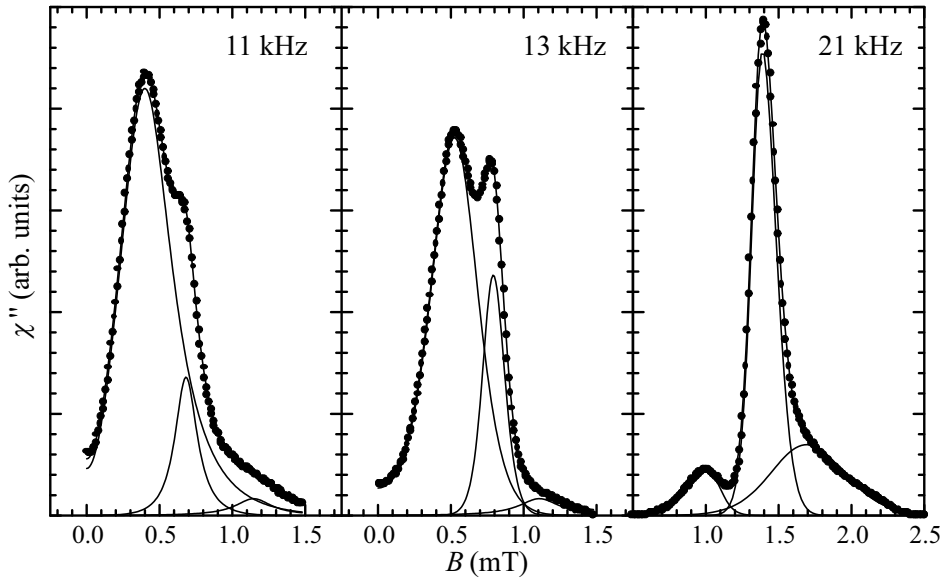


Fig. 2. Decomposition of each first spectra of Fig. 1 to three Lorentz-Gaussian peaks.

it is possible to reproduce asymmetric lines, which are clearly observed at intermediate polarizations. Still, it is not possible to deduce the separate intensities objectively due to the large number of parameters. Therefore, we demanded, in addition, that the two lines must have an equal shape ($B_{L1} - B_{G1} = B_{L2} - B_{G2}$ and $\Gamma_{L1}/\Gamma_{G1} = \Gamma_{L2}/\Gamma_{G2}$), although the positions, widths, and amplitudes do differ. Then the low-field sides of both peaks are fixed by the falling side at the left of the attached pair and the high field sides by the opposite edge. This seemed to be a fair adaptation in all cases analyzed. The physical justification for the particular fitting function is not that essential, since its purpose was just to resemble the data with best possible fidelity to allow accurate determination of partial areas and center positions.

Examples of such processing are shown in Fig. 2 for the highest signals of Fig. 1. We fitted, in fact, three peaks as one can see from the decompositions in Fig. 2. The interpretation of the extended tail, treated as the third peak, will be refined in the context of the isotope effect, as it probably is a reminiscent of the extinguished second isotope line mixed with the effect of varying demagnetization factor over the cross section of the sample. At the frequency 21 kHz, it is natural to associate this additional intensity to the main line, so that the intensity ratio of interest is defined as $I_r = I_1/(I_2+I_3)$. The situation is not as clear, when the line crossing is taking place in the

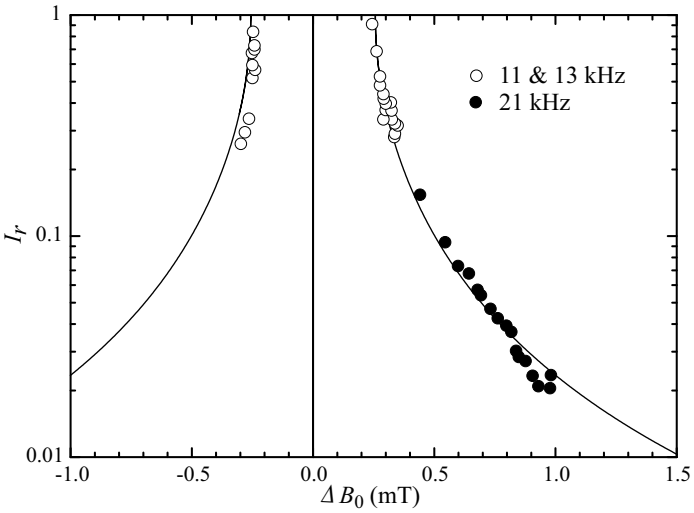


Fig. 3. Intensity ratio of the double-spin mode and the ordinary Larmor line as the function of the separation between the peaks, which evolves with the decreasing nuclear polarization. The lines are theoretical with $f_d = 2.6$ kHz.

other two cases. Fortunately, the third line has then only an insignificant share of the total intensity, so that we chose to ignore it completely. For the data sets at the lowest frequencies, therefore, $I_r = I_1/I_2$ or $I_r = I_2/I_1$, whichever is less than unity. The crossing point is passed, by definition, when $I_1 = I_2$.

The ratios of the intensities in the three measurements are displayed in Fig. 3 An excellent reproduction of the behavior is obtained by using a coupling frequency $f_d = 2.6$ kHz, which is somewhat smaller than the value suggested by Ekström *et al.*[8] No conclusions can be made about the possible polarization dependence of $f_d$.

The resonance positions obtained from the fits and calculated according to our model are shown in Fig. 4. Good agreement is found, in particular at the higher frequency. The steepening of the change of the resonance value of the 21 kHz primary line at the lowest polarizations is due to a remnant of the isotope effect: above about $p = 0.2$ both spin species behave essentially as those with the higher moment (enhanced line), but when approaching $p = 0$, the coupling between the isotopes decreases rapidly and the effective gyromagnetic ratio changes to the average of the isotopes weighted by the abundances. At the lower frequency there is a clear displacement of the primary line from the expected resonance position at low polarizations. It is difficult to assure that this would have any deeper significance, although the difference is somewhat larger than seems plausible to result just from fitting

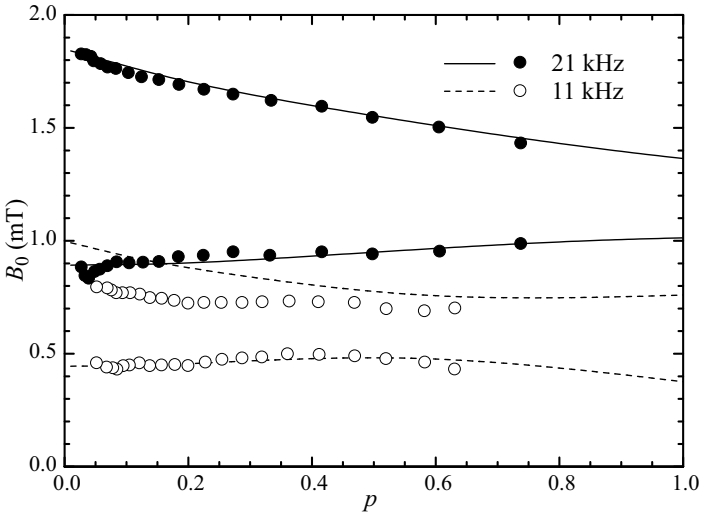


Fig. 4. Resonance positions of the primary and secondary lines at $f = 11$ and 21 kHz as functions of nuclear polarization.

errors.

The double-spin resonance was still resolvable at 111 kHz, see Fig. 5, where we wanted to test if the isotope splitting of the double-spin line would be visible. The sweep in Fig. 5 was started from 0.3 to 0.6 mT, the excitation level was then stepped down by a factor of 10, the main peaks were scanned, and then the sequence was repeated in the opposite order. Due to the long sweep, there was considerable relaxation in the course of the whole episode. The data in Fig. 5 are displayed as measured without subsequent averaging. The signal-to-noise ratio was not good enough for definite conclusions about any structure of the double-spin satellite.

The isotope effect was studied at four different frequencies, 151, 111, 81, and 51 kHz, see Figs. 6 and 7, while still at 21 kHz the suppressed isotope line probably contributed to the tail of the main peak, see Fig. 1. At 81 kHz two measurements were made with the static field either parallel or perpendicular with the sample foils in order to check the effect of grossly different demagnetization factors, see Fig. 7. The change in the relative strengths and the shifts of the peaks are well reproduced, but the measured spectra are much broader than the calculated ones, presumably due to eddy-current screening effects. At the limit $p = 0$ the demagnetization factor makes no difference any more. Some broadening is seen also in Fig. 6 as the frequency is increased. The overall behavior is in accordance with the expectations at all frequencies, but quite interesting small quantitative deviations occur.

The experimental resonance lines were fitted according to the routines

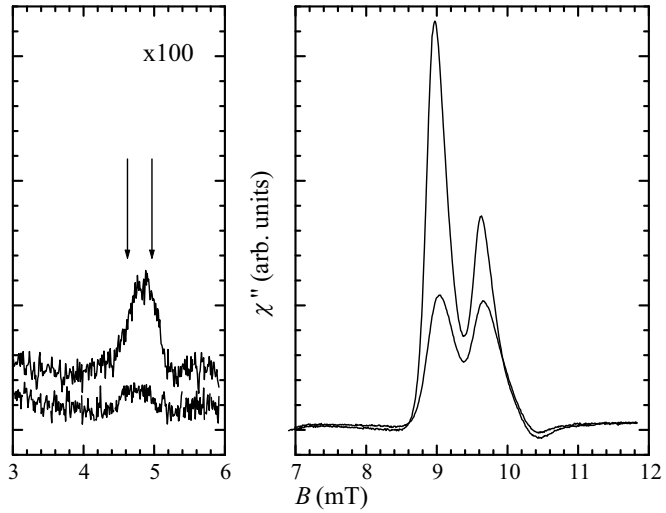


Fig. 5. Double-spin satellite (left) at $f = 111$ kHz, where the main peak (right) already splits into the isotopic lines. The arrows indicate the expected positions for the double flips of like nuclei of either isotope, whereas that of the unlike pairs fits in between. Note the different vertical scales – the double-spin mode is already about 500 times weaker than the Larmor peaks.

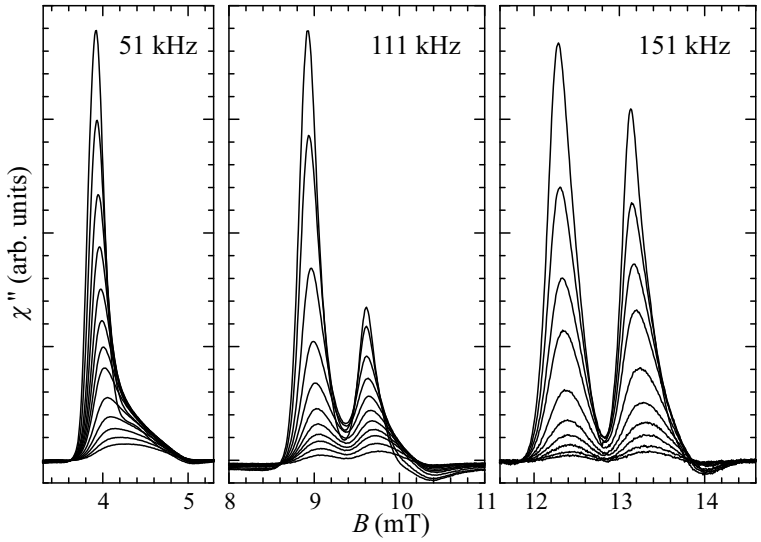


Fig. 6. Measured resonances of copper at $f = 51$, 111, and 151 kHz with the magnetic field parallel to the sample. The isotope effect becomes more dominant toward lower frequencies, so that the upper isotope line is almost extinguished at 51 kHz at high polarizations. The range $p \approx 0.1$–$0.6$ is covered in each panel. Not all measured spectra are shown to improve clarity.

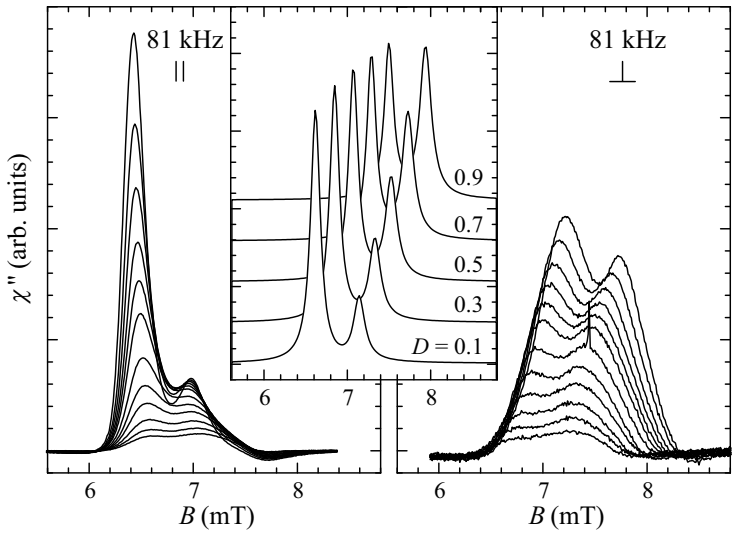


Fig. 7. Measured resonance shapes of copper at $f = 81$ kHz for two different static field orientations. The nuclear polarization varies between about $p = 0.1$–$0.7$ in each run. The inset: calculated spectra at $f = 81$ kHz with $p = 0.7$ for different demagnetization factors between $D = 0.1$–$0.9$ with increments of 0.2. Consecutive spectra have been shifted vertically for better visibility but the horizontal displacements result from the demagnetization effects. The measured spectra at the left panel correspond to $D \approx 0.1$, while the data at the right panel represent the situation with $D \approx 0.9$.

explained above. The ratio of the integrated areas are shown in Fig. 8, while the difference of the first moments of the lines are shown in Fig. 9. These can be compared with the calculated curves. There are obstinate differences between the experimental and computed data, which remain even at the limit of zero polarization and at the highest frequency used in the measurement.

It is particularly difficult to understand the clear deviations seen in Fig. 9, while the resonance positions can be determined very accurately at all but the lowest frequency. We can exclude many possible hypothetical reasons for the steadily too large separation between the interfering isotope modes. Some of the points, which we list below, can be ruled out by the fact that the proposed effect would cause an equal shift for both of the lines (i-iii). Many of the mechanisms would not be active at the limit of zero nuclear polarization (iv-viii). Also, a conflict with the measurements may spring up, since the effect would work to the opposite direction from what we observe (ix) or possibly just distort the line shape but with no net shifts (x). Finally, a potential cause may be considered unlike by requiring modifications to well established quantities (xi). Thus, we enumerate in more detail the following:

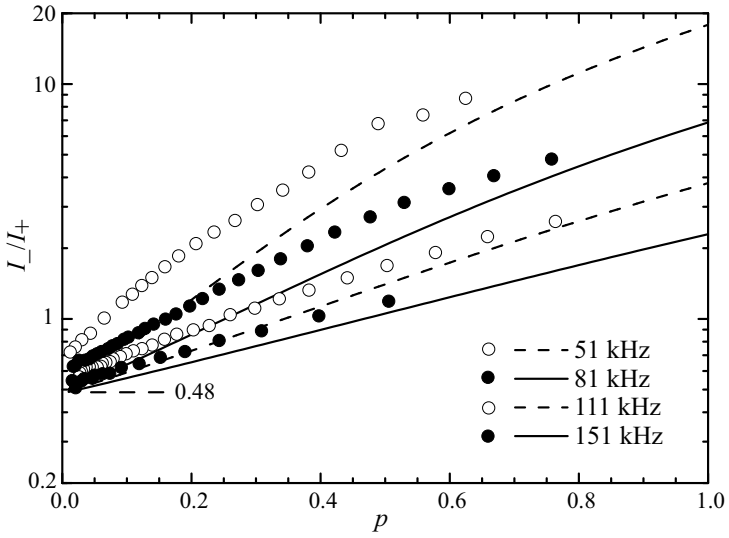


Fig. 8. Relative intensities of the enhanced and suppressed isotope resonances at $f = 51$, 81, 111, and 151 kHz as the function of nuclear polarization. The lines are theoretical curves using $R = -0.42$ without any fitting parameters. At $p = 0$, the intensity ratios should assume the value 0.48 independent of frequency.

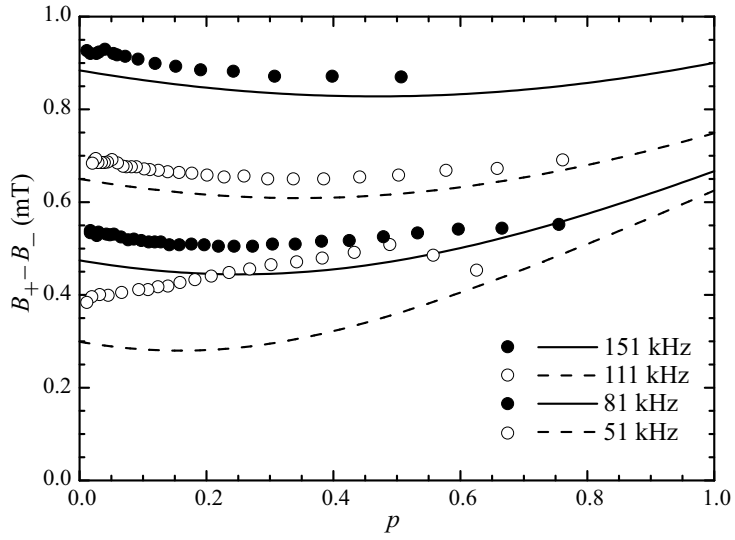


Fig. 9. Separations of the suppressed and enhanced resonance modes at $f = 51$, 81, 111, and 151 kHz as the function of nuclear polarization. The lines are theoretical curves using $R = -0.42$ without any fitting parameters.

i) Erroneous calibration constant for the static field coil is not probable. The field-to-current ratio was fixed according to the $^7$Li resonance and the two copper isotopes *on average* agree with this choice. Further, no unintended static ambient field can cause changes in the *difference* of the positions of the two resonances. Nevertheless, the magnitude of such fields, harmful in many other ways, was checked in separate measurements to remain below 5 $\mu$T in all three coordinate directions.

ii) Errors in the fitting procedure should not be serious, in particular not at the highest frequency and at low polarizations, where the peaks are regular and symmetric in shape, and plenty of spectra could be collected at steady conditions. Errors in the determination of the phase of the signal would give, as a first approximation, equal shifts for both peaks.

iii) Interaction with an unaccounted spin population, such as with electronic paramagnetic impurities, would produce an equal shift in field sweep measurements for both isotopes, as the shift depends rather on the properties of the foreign moments ($\sim R_i\mu_0 h x_i \gamma_i \rho S$, $i$ for impurity with a spin $S$). Furthermore, in pure metals we would probably be dealing with very dilute contaminants, which would couple strongly to the nearby nuclei, but not uniformly to the whole population. Therefore, the effect would probably be just to kick off some fraction of the nuclei from responding at the common resonance frequency, or, as an inhomogeneous effect, to broaden the nuclear-resonance lines.

iv) Erroneous demagnetization factor or the variation of it over the cross section of the sample does not explain the deviations, since the shift persists down to the limit of zero polarization, where the effect of the net interaction fields vanishes.

v) Eddy current effects do give rise to small shifts in the resonance positions, but they should affect both lines by almost equal amounts. Such shifts arise because the penetration depth depends on susceptibility, which is not at all negligible at the resonance at high nuclear polarizations – but being so, this effect should nullify towards zero nuclear polarization.

vi) A pseudo-dipolar interaction, an indirect-exchange term with the dipolar symmetry, which possibly is non-negligible in copper would not produce any observable shifts, as the exchange-type interactions are of short range, and the angular dependence of the dipolar-like interaction nulls the relevant lattice sums within symmetrical spin clusters. Also, as for item iv), the interaction fields vanish as $p \to 0$.

vii) Randomness due to the varying share of like and unlike nuclei as nearest neighbors may produce shifts at finite polarization, because then the dipolar sum does not completely cancel among the nearest neighbors. This effect is presumably small due to only minor difference in the gyromagnetic

ratios, and again, this effect vanishes at zero $p$.

viii) Relaxation effects could produce small shifts during the measurements of the continuously decaying signal. To reduce such problems we swept the field back and forth, and averaged every two consecutive spectra, thus eliminating the distortions due to relaxation in the first order. Also, such complications do not explain the zero-$p$ offsets which are observed under steady conditions.

ix) Line-width effects are in action also at the zero-polarization limit, but their result is always to *attract* the lines irrespective of the sign of the difference of the widths or of the cross-coupling widths. This is because they appear squared in the expression for the coupled mode frequencies. All in all, the line width effects are small in copper, and it is not plausible that we would just be overestimating such effects.

x) Electric quadrupole effects would distort the line shapes symmetrically and so net shift of the lines should not result. Therefore, such hypothesis can be ruled out, although quadrupole effects would indeed be in operation at any $p$.

xi) Of course, a larger separation of the lines could result from erroneous gyromagnetic ratios for the copper isotopes. We do not consider this as a probable cure for the described deviations.

So, we are left speculating, for example, about the role of the higher moments of the spectral lines to the over-all behavior. First of all, it is clear, that the actual line shapes are not really Lorentzian, as is the case for the computed line shapes.

There are some distinct features in the measured signals which may hint about the appropriate solution. First, the intensity between the coupled resonance lines drops remarkably low at the midpoint of the pattern. We have not been able to reproduce such behavior by any reasonable modification of our model. Second, the response is clearly negative at the high field side of the peaks. This is not merely due to a maladjusted phase of the signals, because the susceptibility actually drops negative at *both* sides of the peaks. Such negative contributions make also our intensity analysis less reliable as we do not add any "emission component" to our fitting functions. This was not implemented due to the difficulty of distributing any such negative share objectively between the two lines. Also, to feel comfortable upon including a negative part to the absorption-line shapes, an understanding about its physical origin would be indispensable. When fitting, we simply adjusted the background level so as to coincide with the minimum at the low field side of the resonances. The negative contributions may, of course, give some bias also to the determination of the first moments of the lines, but once again, this effect becomes negligible at low nuclear polarizations and it also

becomes less severe at lower frequencies.

Putting aside the unaccounted overall shift, the calculations mimic fairly well the behavior of the line separation as the function of polarization. In particular, the position and depth of the minimum in the separation, which occurs in the course of the measurements are reproduced with a reasonable fidelity. The minimum results from the higher field line, primarily of $^{63}$Cu, moving faster downwards as a function of increasing polarization than the other line at the lower field, until the repulsion between the modes overcomes this approaching.

The ratio of the fitted intensities is systematically higher than we compute, see Fig. 8. Most notably, the intensity ratio at $p = 0$ does not quite settle to the value deduced from the ratio of the abundances and the gyromagnetic ratios, $(x_{65}\gamma_{65})/(x_{63}\gamma_{63}) = 0.48$. The deviation becomes progressively larger as the frequency is lowered. In fact, almost perfect compatibility would be achieved by multiplying the theoretical curves at each frequency by constants between 1.1 and 1.5. The overall agreement between the theory and the experiment could not be improved by altering the exchange constant $R$, as this would mainly just change the steepness of the curves.

The discrepancies in the intensity ratios are obviously at least partly due to the same unknown effect that contributed to the separations between the modes. However, the first guess for its influence on relative intensities would be the opposite to what we actually see. As the lines move further apart from each other, one would expect the interference effect on the intensities to diminish. We are then led to reason the opposite: there is interference between the lines even at very low polarizations, which is seen also as an additional repulsion between the lines. These anomalies are thus more likely of internal rather than of external origin.

We hesitate on making any definite statements about the intensity ratios because of the already mentioned difficulties in the quantitative analysis of the closely residing peaks. When fitting the lines we have used here a fixed ratio for the widths of the two peaks. This is fully justified at the higher frequencies, where freeing this restriction does not make any changes on the results. Quite naturally, we chose the fixed-width ratio on the basis of such fitting series. At lower frequencies, however, the extinguishing mode appears to become broader at high polarizations, tempting to allow variation of its width. We make no exception here, though, because we may actually see a superposition of several effects. It is obvious, that a contribution to the extended tail on the high-field side at low frequencies and high polarizations is produced by variation of the demagnetization factor over the cross section of the sample. The majority of the nuclei feel the small $D$ and resonate uniformly at lower (than Larmor) fields, but close to the edges of the sample

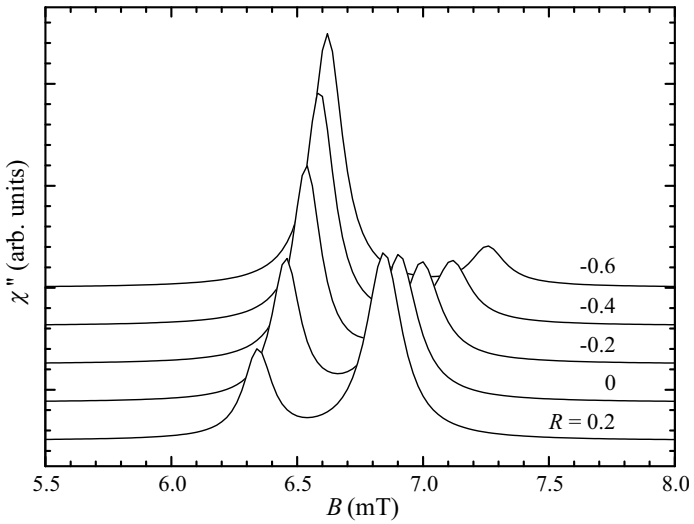


Fig. 10. Computed spectra for copper at $f = 81$ kHz and $p = 0.7$ assuming different values for $R$. Consecutive spectra have been shifted vertically for better visibility but the horizontal displacements result from the changing $R$.

$D$ deviates ostensibly (in a continuous fashion, of course) from the bulk value: where $D \sim 0.3$, nearly no dipole shifts occur, while in regions with $D > \frac{1}{3}$ to the extreme corners ($D = 1$) positive shifts must exist. The net effect is an extended trail which may well resemble those seen at 21 and 51 kHz, see Figs. 1 and 6. At lower polarizations the shifts diminish and the lines themselves become broader so that the tail effect is expected to disappear.

Finally, we may demonstrate the sensitivity of the isotope effect on $R$ by plotting a series of spectra with this parameter varied at a constant polarization, see Fig. 10. Not much changing is needed to turn the suppression-enhancement effect the opposite to what is observed in the experiments.

The conclusion after all this discussion is that the exchange constant adopted by Ekström *et al.* on the basis of their measurements on the isotope effect at 183 kHz and on the double-spin effect below 1.5 mT, $R = -0.42 \pm 0.05$, is in good agreement with our new measurements. We extended the observations of the double-spin mode up to about 5 mT and studied carefully the isotope effect over a wide range of frequencies. Persistent unexplained deviations from the expected behavior were pointed out.

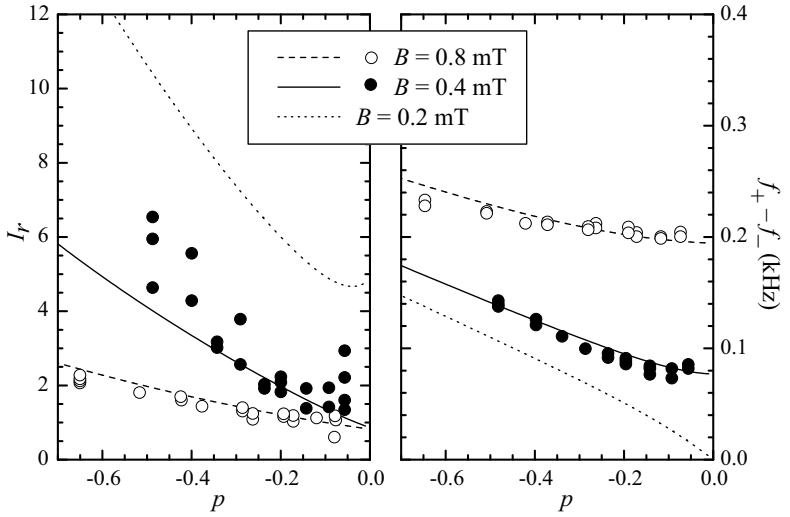


Fig. 11. Comparison of our calculations with the measurements on silver at negative absolute temperatures. The data is taken from Ref. 9. There are no experimental points at 0.2 mT, since the suppression factor of the weaker line was too large for reliable analysis.

### 3.2. Silver

Silver is dominated by the indirect exchange interaction with $R = -2.5$. Attempts to observe the second harmonic line have not been successful, which is understandable due to the mechanism increasing the width difference and thus suppressing the relative intensity of the double-spin satellite, when $|R|$ is large, as explained in Sec. 2.1.

Silver has two isotopes $^{107}$Ag and $^{109}$Ag with $x_{107} = 0.52$ and $x_{109} = 0.48$, with $\gamma_{107} = 1.72$ MHz/T and $\gamma_{109} = 1.98$ MHz/T, and with $I_{107} = I_{109} = \frac{1}{2}$. The isotope effect is remarkably clear due to the relatively high value of $R$. Most thorough published data on silver have been measured at negative nuclear polarizations at the range $p = -0.7$–$0$.[9]

We merely recalculate the intensity ratios and resonance frequencies using our formulae in Eqs. (14) and (16), the outcome of which is shown in Fig. 11. The agreement with the measurements is satisfactory without any parameters adjusted. Some features of the data at either field could be better reproduced by tuning the coupling constants slightly but the overall agreement would not be much improved. In particular the difference of the resonance frequencies may have a minimum at small negative polarization in $B = 0.4$ mT, which could be reproduced by such manipulation.

In Fig. 12 we show a decomposition of a pair of resonance lines into

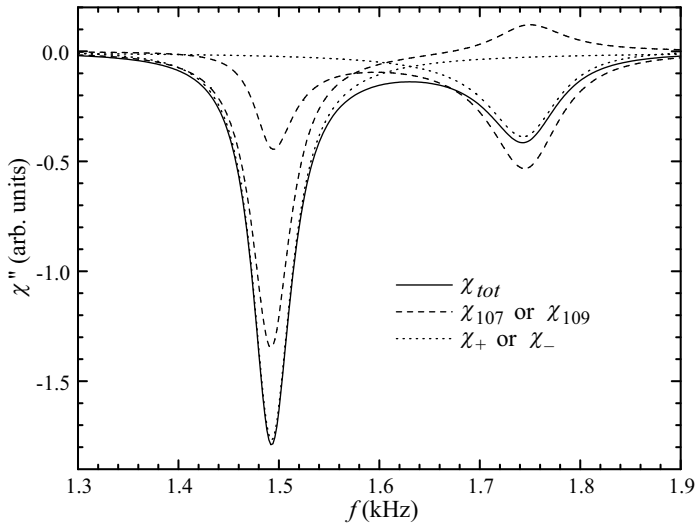


Fig. 12. Decomposition of a resultant spectrum of silver at $p = -0.683$ in $B = 0.822$ mT into its isotopic contributions $\chi_{107}$ and $\chi_{109}$ (dashed lines). Also the coupled modes $\chi_+$ and $\chi_-$ are shown separately (dotted lines). The full spectrum is the sum of either pair of these: $\chi_{tot} = \chi_{107} + \chi_{109} = \chi_+ + \chi_-$ (solid line). The corresponding measured spectrum can be found in Ref. 9.

$\chi_{107}$, $\chi_{109}$, $\chi_+$, and $\chi_-$. The features discussed in Sec. 2.2 are clearly visible and the resultant line shape is in excellent agreement with the real measured data.[9]

What comes to the data at 0.2 mT, see Ref. 9, there really is merging of the lines essentially at zero polarization only. The interference satellite is not observed experimentally at finite polarizations simply because the suppression factor is so large. The calculated line shape at the frequency interval of the actual measurement shows just a slightly elevated background level at the high frequency side, which is easily nulled by a little maladjustment of the phase of the signal. According to our analysis there is line crossing below $B \approx 0.27$ mT at very small positive polarizations ($p < 1\%$), but no significant changes of the line shape take place at the crossing point.

We conclude that the earlier adopted parameter values for silver are in full accordance with our analysis. The good agreement between the model and the actual data is at least partly explained by the fact that the measured line shapes are very close to Lorentzian as are the resonances obtained from the linear equations of motion introduced in this paper.

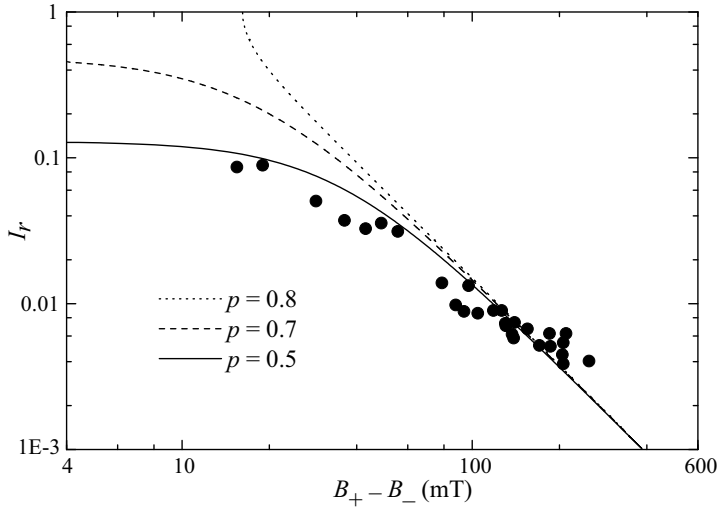


Fig. 13. Measured intensity ratios of the double-spin mode compared to the Larmor line of rhodium at $p \approx \pm 0.5$ at different frequencies between $f = 130$–$830$ Hz. Theoretical curves are shown for different polarizations.

### 3.3. Rhodium

We shall critically reexamine the data on the double-spin effect in rhodium.[11] The conclusion about the magnitude of exchange, $R = -1.0$, based on the shifts of the double-Larmor mode, is not altered but the intensity analysis and the behavior close to the line crossing require some further attention.

The relative exchange constant is more than twice as large as in copper, and it is evidently just enough to change the system from exhibiting non-crossing ($f_d > \delta_d$) to crossing ($f_d < \delta_d$) behavior of the double-spin mode. Since this is a line-width effect, it depends on polarization ($\delta \propto (1-p^2)$), and the non-crossing condition should be regained at high enough polarizations. Such change is estimated to take place at about $p = 0.8$ in rhodium.

We plot the relative intensities of the two modes in Fig. 13, where the Gaussian fitted data[11] for the double line are reproduced. Along with the data three theoretical curves calculated for $p = 0.5$, 0.7, and 0.8 with $f_d = 23$ Hz and $\delta_d(p = 0) = 51$ Hz are shown. The polarization dependence of the relative intensities at the vicinity of the line crossing stems from the changing line widths, which was not accounted for in the original paper by Tuoriniemi *et al.*[11] The line-crossing condition is signalled by the extrapolated intensity ratio intercepting the vertical axis at zero separation, while the non-crossing of the lines at higher polarizations results in equal intensities for the modes

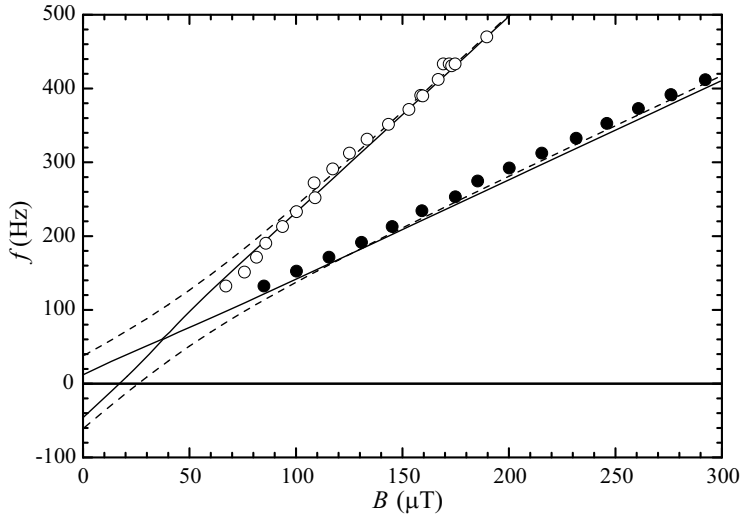


Fig. 14. Measured resonance positions of the double-spin mode and the Larmor line in rhodium at $p \approx +0.5$. Improved theoretical curves showing a crossing behavior are shown as solid lines.

with a finite separation. The opening up of a gap between the modes at the crossing field $B_\times$ is illustrated in more detail in Figs. 14 and 15.

The revised theoretical coupled mode frequencies for $p = 0.5$ are plotted together with the data in Fig. 14. The improved compatibility is evident, and the persistent approaching of the two modes is reproduced without any difficulty. Below the points plotted, there is just one peak observed in the experiment. The double-peaked structure, as seen in copper, does not appear because the double-spin line remains weak (at low p) and sits more or less on top of the main line.

Fig. 15 shows the resonance frequencies close to and beyond the critical polarization, at which the repulsion between the modes overcomes the merging tendency. Some simulated resonance lines as the function of polarization around the crossing field $B_\times(p = 1) = 0.07$ mT at the frequency $f = 0.11$ kHz are shown also. Unfortunately, the measurements at the line-crossing region did not extend to high enough $p$ in order to attest such evolution experimentally.

Finally, we can compare the values for $f_d$ obtained for the two metals, copper and rhodium. The experimental ratio is $2.6/0.023 = 110$, while the expected scaling gives $\frac{\mathrm{Cu}}{\mathrm{Rh}}[\gamma^2\rho\sqrt{I(I+1)}] = 190$. The consistency, although not perfect, is improved from the earlier estimates.[11]

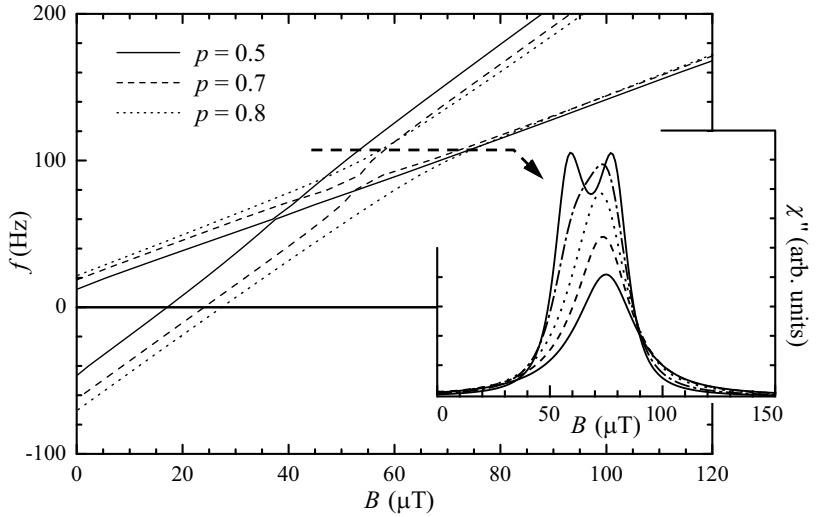


Fig. 15. Transition from the crossing to non-crossing behavior in rhodium as the function of polarization. The computed spectra at $f = 110$ Hz, overlaid on the plot, show a distinct change of shape as the polarization increases: $p = 0.55$, 0.65, 0.75, 0.85, and 0.9, from the smallest to the double-peaked spectrum.

### 3.4. Thallium

Thallium has two isotopes with 30%/70% abundances and with gyromagnetic ratios very close to each other. The peculiar line-splitting behavior observed at high nuclear polarizations[13] led Oja *et al.*[14] to propose that it results from the isotope effect. By comparing the calculated separation and intensities of the two modes with the experimentally observed ones, we must conclude that this explanation cannot be correct. This is decisively so, although the values for the nuclear polarization, where the exchange merged line is expected to split, is close to where the anomaly was seen experimentally. In a later paper by Heinilä and Oja the authors make a statement parallel to this.[19]

To clarify why conclusions based only upon the appearance of two modes as eigenfrequencies of the system may lead to erroneous interpretation, we point out that even in the case of just one single isotope, with all magnetic moments exactly equal, one obtains two modes at finite polarizations, if the spins are just fictitiously divided into two populations and labelled differently. It must be realized, though, that all intensities of the second "fictitious" mode are exactly zero, and there exists no multiple peaks after all. If this is overlooked and one adds to the description a merging term

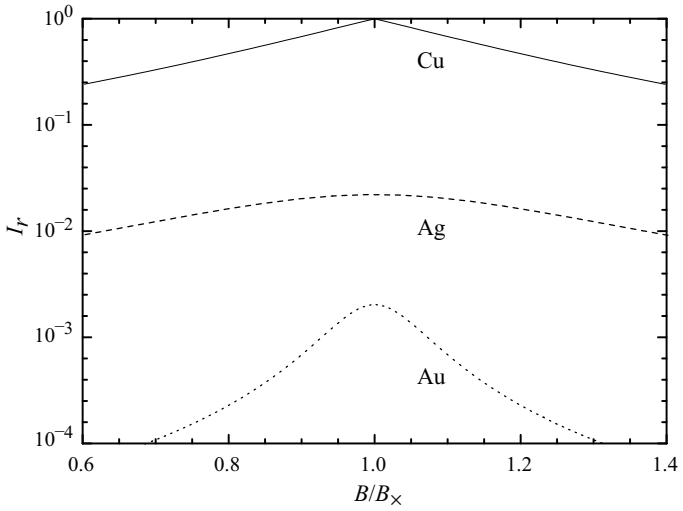


Fig. 16. Estimated relative double-spin resonance intensities for the three noble metals at $p = 0.9$ as functions of the magnetic field normalized by $B_\times$, individual for each metal.

competing with the line splitting, one obtains the behavior described by Oja *et al.*[14]

More probable cause for the structure of the thallium resonance at high nuclear polarization is due to eddy-current effects in the metallic sample.[20] Pulse-NMR with large tipping angles was used under circumstances where the penetration of the field was not complete. This leads to complicated and interesting effects as the penetration depth depends on susceptibility. This, in turn, has a nuclear contribution, which is not at all negligible at high degree of polarization and at the vicinity of the resonances, where small excitation fields give rise to a large transverse magnetization ($\equiv$ high susceptibility). As the magnetization is spurred to precession with varying drive across the depth of the sample, this can lead to a complicated fine structure of the resonance lines.[20]

### 3.5. Gold

There exist no published data on gold, so we pass by this section by just reevaluating the relative double-line intensities for the three noble metals – Cu, Ag, and Au – following the example of Moyland *et al.*,[15] see Fig. 16. The intensity ratio in Au is desperately small in all magnetic fields, and so the only way to have any chance of observing this phenomenon is to use

some indirect methods, as proposed in Ref. 11.

### 3.6. Lithium

Lithium metal has some exceptional properties, which we want to point out. First, the abundances of the two isotopes are quite uneven, $x_7 = 0.92$ and $x_6 = 0.08$, and, in particular, the difference between the gyromagnetic ratios is uncommonly large, $\gamma_7 = 16.5$ and $\gamma_6 = 6.3$ MHz/T. Also the spin quantum numbers differ: $I_7 = \frac{3}{2}$ and $I_6 = 1$. It will be interesting to learn if the two effects discussed here indicate the same value for the exchange constant $R$, while the double-spin method probes exclusively the exchange between like nuclei and the isotope effect quite contrary that between unlike nuclei. At any rate, the indirect exchange is expected to be rather weak, $|R| \ll 1$, and presumably ferromagnetic. Such a crude estimate can be made on the basis of the large Korringa constant, 45 sK, indicating weak coupling between the nuclear spins and the conduction electrons. The positive sign is predicted by the free electron model of Ruderman and Kittel.[5]

As a final note we can speculate about the possibility of a direct exchange between $^7$Li nuclei. We are dealing with one of the lightest isotopes, and consequently, the zero-point vibrations have a reasonably large amplitude, of the order of 10% of the lattice spacing. The lithium lattice is too stiff to allow any tunnelling contribution, but the exchange due to the Coulomb repulsion might be marginally perceptible.[21] Such direct-exchange effects are decisive for the nuclear-magnetic ordering in solid $^3$He around 1 mK. Interestingly, the more abundant Li nuclei are fermions whereas the lighter ones are bosons. Therefore, the direct exchange is relevant for the heavier isotope only and any observed difference between the exchange constants of the two isotopes may be an indication of such effects.

It is too early to present any actual results on lithium in this paper, but we have indeed observed both the double-spin effect on $^7$Li and also a weak isotope effect between the two spin species.

## 4. CONCLUSIONS

We have discussed two NMR phenomena characteristic for polarized spins, which allow an exclusive experimental determination of the exchange-type coupling between the nuclear moments. When the exchange term is weak or moderate compared to the dipolar coupling, the exchange parameter $R$ is most reliably found by examining the shift of the double-spin mode as the function of nuclear polarization. For large values of $R$, the broadening

of the secondary line reduces its relative intensity easily beyond the limits of experimental resolution. In such cases, the existence of two or more isotopes with a non-zero nuclear spin, if so fortunately occurs, gives an opportunity to study the so-called suppression-enhancement effect of the isotopic lines. This is an interference phenomenon between the different spin populations, and depends strongly on the coupling parameter $R$ thus allowing its accurate determination.

We presented here a uniform description of both of these effects on the basis of the equations of motion for the spin operators. We reviewed the application of these methods to several pure metals and reanalyzed some of the data by our improved formulations. We presented new extended data on copper and pointed out some remaining inconsistencies with the proposed description.

## ACKNOWLEDGMENTS

This research was supported by the Academy of Finland (Finnish Centre of Excellence Programme 2000-2005) and by the European Union (Large Scale Installation Program ULTI-III, HPRI-1999-CT-0050). KJ appreciates the support by Finnish National Graduate School in Material Physics.

## REFERENCES

1. A.S. Oja and O.V. Lounasmaa, *Rev. Mod. Phys.* **69**, 1 (1997).
2. A. Abragam and M. Goldman, *Order and Disorder*, Clarendon press, Oxford (1982).
3. See *e.g.* V. Bouffard, C. Fermon, J.F. Gregg, J.F. Jacquinot, and Y. Roinel in *NMR and More*, p. 81, Edited by M. Goldman and M. Porneuf, Les Editions de Physique, Les Ulis (1994), and references therein.
4. See *e.g.* Y. Karaki, M. Kubota, H. Ishimoto, and Y. Ōnuki, *Phys. Rev. B* **60**, 6246 (1999), and references therein, H. Ishii, *this issue*.
5. M.A. Ruderman and C. Kittel, *Phys. Rev.* **96**, 99 (1954).
6. M.T. Huiku, T.A. Jyrkkiö, J.M. Kyynäräinen, A.S. Oja, and O.V. Lounasmaa, *Phys. Rev. Lett.* **53**, 1692 (1984), A.J. Annila, K.N. Clausen, A.S. Oja, J.T. Tuoriniemi, and H. Weinfurter, *Phys. Rev. B* **45**, 7772 (1992), H.E. Viertiö and A.S. Oja, *Phys. Rev. B* **48**, 1062 (1993).
7. T.A. Jyrkkiö, M.T. Huiku, O.V. Lounasmaa, K. Siemensmeyer, K. Kakurai, M. Steiner, K.N. Clausen, and J. Kjems, *Phys. Rev. Lett.* **60**, 2418 (1988), A.J. Annila, K.N. Clausen, P.-A. Lindgård, O.V. Lounasmaa, A.S. Oja, K. Siemensmeyer, M. Steiner, J.T. Tuoriniemi, and H. Weinfurter, *Phys. Rev. Lett* **64**, 1421 (1990), J.T. Tuoriniemi, K.K. Nummila, R.T. Vuorinen, O.V.

Lounasmaa, A. Metz, K. Siemensmeyer, M. Steiner, K. Lefmann, K.N. Clausen, and F.B. Rasmussen, *Phys. Rev. Lett* **75**, 3744 (1995), M. Steiner, *this issue*.
8. J.P. Ekström, J.F. Jacquinot, M.T. Loponen, J.K. Soini, and P. Kumar, *Physica* **98B**, 45 (1979).
9. P.J. Hakonen, K.K. Nummila, and R.T. Vuorinen, *Phys. Rev. B* **45**, 2196 (1992).
10. A.S. Oja, A.J. Annila, and Y. Takano, *J. Low Temp. Phys.* **85**, 1 (1991).
11. J.T. Tuoriniemi, T.A. Knuuttila, K. Lefmann, K.K. Nummila, W. Yao, and F.B. Rasmussen, *Phys. Rev. Lett.* **84**, 370 (2000).
12. A.S. Oja, A.J. Annila, and Y. Takano, *Phys. Rev. Lett.* **65**, 1921 (1990).
13. G. Eska and E. Schuberth, *Jpn. J. Appl. Phys.* **26** Suppl. 3, 435 (1987).
14. A.S. Oja, A.J. Annila, and Y. Takano, *Phys. Rev. B* **38**, 8602 (1988).
15. P.L. Moyland, P. Kumar, J. Xu, and Y. Takano, *Phys. Rev. B* **48**, 14020 (1993).
16. H. Cheng, *Phys. Rev.* **124**, 1359 (1961).
17. J.H. Van Vleck, *Phys. Rev.* **74**, 1168 (1948).
18. W. Yao, T.A. Knuuttila, K.K. Nummila, J.E. Martikainen, A.S. Oja, and O.V. Lounasmaa, *J. Low Temp. Phys.* **120**, 121 (2000).
19. M.T. Heinilä and A.S. Oja, *Phys. Rev. B* **50**, 15843 (1994).
20. G. Eska, *private communication* (2003).
21. See *e.g.* R.A. Guyer and L.I. Zane, *Phys. Rev.* **188**, 445 (1969).